Engineering a Universal Dengue Virus Vaccine using a Virus-Like Particle Scaffold

Danielle A. Basore[1,3], Carolyn M. Barcellona[2], Thomas B. Jordan[1, 5], Donna E. Crone[1], Sharon Isern[2,4], Scott F. Michael[2], Christopher Bystroff[1]

[1]Biological Sciences, Rensselaer Polytechnic Institute, Troy, NY, USA, [2]Biological Sciences, Florida Gulf Coast University, Fort Myers, FL, USA, [3]Mercy College, Dobbs Ferry, NY, USA. [4]Center for Scientific Review, National Institutes of Health, Bethesda, MD USA. [5]Charles River Labs, Wilmington MA, USA.

Abstract

The fusion loop (FL), a 51-residue segment of the dengue virus (DENV) envelope (E) protein, has been shown to bind antibodies that neutralize DENV infection in cell culture. Vaccination with this loop could raise broadly neutralizing antibodies and avoid antibody dependent enhancement in second serotype infections associated with whole virus vaccination. We propose a new DENV vaccine in which FL has been genetically fused to a well-known and highly immunogenic carrier, the human papillomavirus (HPV) L1 protein (L1). Chimeric L1-FL was expressed in human cell culture, but expression levels of virus-like particles (VLP) were initially low. Expression levels were improved after adding a bridging disulfide bond at the base of the loop, and were further improved by transfecting cells with a mixture of 9 parts chimera to 1 part wild-type L1 expression vectors. VLPs formed from the chimeric construct were purified using ultracentrifugation and were shown to form hollow particles of the expected size using transmission electron microscopy. The improvements in expression are discussed in the context of a theoretical pathway for folding and assembly of VLPs.

1 | INTRODUCTION

Viruses affect all domains of life, and so many organisms have evolved mechanisms to detect and respond to viral capsids[1–3]. In vertebrates these mechanisms, including activation of toll-like receptor 4[4], size selective entrance into the germinal centers of the lymph nodes[5], and recognition of the highly multivalent structure that enhances avidity to the maturing B-cells[6], all make viral capsids efficient immunogens.

Human papilloma virus (HPV) L1 protein self-assembles into highly stable T=7 icosahedral 55 nm VLPs, identical in structure to the natural HPV capsid[7,8]. The VLPs each consist of 360 copies of L1, arranged in 72 pentamers, called capsomeres, which contain no other DNA or protein and are stabilized by multiple internal and inter-unit disulfide bonds. Because HPV infection is associated with the development of certain cancers, L1 VLPs are widely used as anti-cervical cancer vaccines[9].

L1 can fold and form VLPs despite mutations in certain surface exposed loops. Specifically, up to 39 residues of HPV L2 protein have been inserted at position 137 (DE loop) in L1 of HPV Type 16, without disrupting VLP formation or stability[10]. The HPV L1 monomer has a greek key or jelly roll fold, with a well-studied, theoretical folding pathway that provides guidance when considering the effect on folding of inserted antigenic loops[11–14]. One loop in particular, called the DE loop is predicted to fold late in the monomeric folding pathway, explaining the tolerance for insertions at this location[15]. The ability to genetically insert peptide antigens into HPV L1 VLPs provides an opportunity to use the immunogenicity of VLPs to create multifunctional vaccines and focus immunity toward neutralizing epitopes by inserting specific sequences into L1[16].

DENV is a tropical virus spread primarily by two mosquito vectors, *Aedes aegypti* and *Aedes albopictus*. Climate change and globalization have spread the vectors, and therefore the virus, whose clinical manifestations range from mild flu-like symptoms, rash, and joint pain, to dengue hemorrhagic fever (DHF) or dengue shock syndrome (DSS). Exposure to any one of DENV's four known serotypes does not provide cross-protective immunity to the other three. On the contrary, infection with a second serotype can result in the very severe conditions DHF and DSS through the process of antibody dependent enhancement (ADE) of infection, a phenomenon that occurs when antibodies from the first infection bind

weakly to the viral particles of the second serotype, and target the still infectious viral particle to macrophages and other Fc receptor-bearing cells that are normally not infected[17]. A global estimate from the WHO estimates 390 million DENV infections, half a million hospitalizations and approximately 12,500 deaths annually, making dengue one of the most prevalent vector-borne diseases in the world[18]. While there is a tetravalent vaccine available for dengue, it uses the full-length DENV envelope (E) surface protein and elicits an enhancing antibody response that can result in more severe outcomes in naïve recipients when they are exposed to DENV[19]. Consequently, use of this vaccine has been discontinued in many countries or is only licensed for use in people older than nine who have already experienced one or more DENV infections. The development of a safer dengue vaccine that does not induce enhanced disease is a high priority.

A subunit vaccine that focuses immunity specifically against neutralizing epitopes of DENV may avoid vaccine-induced ADE. A broadly neutralizing epitope has been identified by localizing the binding sites of broadly neutralizing monoclonal antibodies derived from patients post-DENV infection[20]. These antibodies blocked the fusion of the virus with the endosomal membrane within the infected cell, severing the life cycle of the virus[21]. The antibody binding is conformationally dependent and negatively affected by mutations within the neutralizing epitope, confirming that the neutralizing antibodies bound to that site. The neutralizing epitope encompasses the part of domain II of the envelope (E) protein of DENV, referred to as the fusion loop (FL), which is highly conserved. During infection, the DENV E protein undergoes a dramatic conformational change upon exposure to low pH, visible in TEM images[22], producing a trimeric spike that exposes the hydrophobic FL and triggers fusion between the viral and endosomal membranes[20]. However, designing such a subunit vaccine is not trivial. Here we demonstrate proof of principle of the protein design elements of a hypothetical vaccine candidate by inserting the DENV FL into an exposed loop of HPV L1, creating a chimeric VLP containing parts from two antigenic proteins from different viruses. Considerable further work would be required to ascertain if these VLPs could induce a useful immune response.

2 | RESULTS

2.1 | Design of constructs

Two different chimeric proteins were designed and produced. In both, two adjacent HPV L1 residues, A137 and N138 in the DE loop were removed to create space and replaced with DENV E protein residues. In the initial chimera (designated FL), the DENV FL insert consisted of a 55 amino acid consensus from the four serotypes of DENV, flanked on each side with a glycine residue to allow flexibility. The second chimera was designed by modeling experiments using the crystal structures of HPV 16 L1 (PDB id 2R5H) and DENV serotype 2 E protein (PDBid 1OAN, Accession AHB63923). This approach resulted in the insertion of 51 amino acids from DENV serotype 2 E protein, flanked by upstream CGP and downstream GPC motifs, creating a new potential disulfide at the base of the DENV E insert. This second chimera was designated cysFL to reflect the design of the cysteine disulfide at the base of the DENV E insert. CGP/GPC linkers have been used to stabilize the display of short peptides on the surface of the enzyme thioredoxin on the surface of bacteria for the purpose of high throughput screening[23]. By adding CGP/GPC to the interface between the L1 and the FL insert, we encourage the formation of a disulfide bond that produces topological isolation (i.e., "pinching" off) of the FL insert. This decreases the effect of the additional loop entropy and encourages the proper folding of both the L1 monomer and FL insert[24]. The pair of flexible Gly-Pro dipeptides is believed to isolate, to some extent, the folding of the FL from the folding of L1, making both more efficient. Amino acid sequences of both chimeras and a model for the resulting structure are shown in Figure 1.

2.2 | Expression of recombinant proteins

The expression of the constructs was confirmed by Western blot analysis of equal amounts of the denatured cell lysates of each transfection probed with CAMVIR-1 anti-HPV L1 Ab (Figure 2). The wild type L1 band can be seen at approximately 55 kDa. The chimeric L1 bands, L1-FL or L1-cysFL, are slightly higher at approximately 61 kDa, because of the inserts. L1-FL expression was only one tenth of the level of L1-WT, indicating that this chimera is less stable than the WT L1 protein. The expression of the CGP/GPC FL

construct, L1-cysFL, was approximately 3-fold higher than for L1-FL, indicating that this chimera showed increased stability compared to the initial L1-FL construct, but was still somewhat less stable than WT.

2.3 | Confirmation of L1-FL expression in the cytoplasm

Images of transfected 293TT cells provide visual confirmation of expression of GFP in green (Figure 5). Red fluorescence shows L1 protein expression bound to CAMVIR-1 anti-HPV L1 antibody. Overlapping fluorescence (orange) indicates that both GFP and L1 proteins are expressed in the same cell, although this does not always occur because the plasmid has separate promoters. Peri-nuclear L1 fluorescence shows that the L1 protein remains in the cells and not in the supernatant. Binding was not observed with the conformationally sensitive anti-FL monoclonal antibody 1.6D[20] with either the L1-FL or L1-cysFL constructs, possibly due to the chimeric FL not being folded correctly in the cytoplasm because the disulfide bonds have not yet formed.

2.4 | Characterization of assembled VLPs by ultracentrifugation

Rate zonal ultracentrifugation conditions were selected to discriminate between unassembled, assembled and aggregated L1 proteins in equal amounts of cell lysates. Following centrifugation, nine equal volume fractions were collected from the bottom to the top of the centrifuge tube and assayed by Western blot. VLPs appear in the middle fractions (2-8), while fraction 1 consists of aggregates that sediment to the bottom of the tube and fraction 9 is unassembled monomers or capsomeres that do not enter the gradient. Results of these experiments are shown in Figure 3. Wild type HPV L1 (L1-WT) VLPs sediment to fractions 4 - 6, suggesting that they form uniformly sized particles. L1-FL enters the gradient but appears in equally low quantity in all fractions with no discernable peak, indicating that assembly of these particles is reduced and is not uniform. L1-cysFL VLPs express and assemble better overall than the uncrosslinked counterpart and sediment mostly to fractions 6 and 7, corresponding to a uniform but less dense VLP than the wild type, likely due to the increased hydrodynamic diameter of the particles with the addition of the inserted FL.

Additional transfection experiments were performed to investigate if co-expression of a small amount (1:9) of WT L1 could rescue the expression and assembly of the chimeric L1-FL and L1-cysFL proteins. Western blot analysis showed that expression and VLP formation are improved for both L1-FL and L1-cysFL in the presence of WT L1. Interestingly, the ratio of L1-FL to L1-WT in these middle fractions is approximately 1:1, even though 9:1 of plasmid was transfected, indicating that even in the presence of WT L1, L1-FL has reduced stability and may be degraded or aggregate. Co-expression of WT L1 appears to stabilize and promote assembly of the L1-cysFL VLPs to near WT levels.

2.5 | Analysis of VLPs by transmission electron microscopy

Wild type HPV 16 particles produced by expression of L1 in HEK 293TT cells and purified by ultracentrifugation are visible with uranyl acetate staining (Figure 4). They are roughly spherical and approximately 55nm across, indicating properly folded protein and assembled particles. Additionally, purchased HPV 18 L1 particles also appear similar to HPV 16 L1 VLPs. The chimeric L1-cysFL samples display hollow 55 nm spheres but without clear capsomere segmentation. We speculate that the FLs, being much larger than the native DE loop, obscure the capsomere boundaries. We were not able to observe VLPs of the L1-FL chimera by TEM.

2.6 | Confirmation of correctly folded and accessible DENV FL in VLPs

An ELISA was used to probe chimeric, assembled VLPs for correctly folded DENV FL (Figure 6). High bind 96 well plates were coated with VLPs and probed with a conformationally-sensitive human anti-DENV FL Ab (1.6D), followed by goat anti-human IgG HRP. Increasing concentrations of hMAb 1.6D bind specifically to L1-cysFL VLPs in a dose-dependent manner, but not to WT VLPs. This indicates that the FL in chimeric L1-cysFL VLPs is properly folded, exposed, and accessible to an anti-DENV FL antibody when bracketed by the CGP/GPC motif.

3 | DISCUSSION AND CONCLUSIONS

The challenge in expressing a chimeric VLP is that success depends on spontaneous protein self-organization at multiple distinct levels, capsid monomer folding, pentamer (capsomere) formation from monomers, formation of the super-quaternary structure of the icosahedral particle from capsomeres and

folding of the insert, any of which may be disrupted by the fusion of the different viral proteins. Our initial attempt utilizing a DENV FL sequence flanked by glycines (L1-FL) did not express at high levels and did not assemble efficiently into VLPs. An inserted loop could produce this result via two likely mechanisms- entropic effects in folding or steric effects in oligomerization. An entropic barrier to folding may have been introduced when the DENV FL was inserted into the L1 DE loop, increasing the contact order[25] of that loop and possibly slowing its folding. The results are consistent with a FL whose folding is controlled by free energy and which, because of its smaller size, folds much faster than L1. We pursued two different strategies to overcome this limitation: redesign of the FL insert site and coexpression with a small amount of WT L1. Both strategies were successful in stabilizing the chimeric protein and improving assembly of chimeric VLPs.

As viral structural proteins, HPV L1 and DENV FL are both heavily disulfide crosslinked for stability. We reasoned that the presence of an additional disulfide at the base of the FL insertion site might effectively lock the FL in its folded state and separate it's folding from L1. We propose that the designed covalent crosslink in L1-cysFT returns the L1 DE loop conformational entropy to its approximate wild-type value, allowing L1 to fold at its native rate or at a more native-like rate. Molecular modeling did not show steric interference between FL and L1, despite the 51-residue size of the FL in the L1-cysFL construct. Experimental results showed that bracketing the FL insert with a disulfide containing CGP/GPC motif improved expression and VLP assembly.

Coexpression of defective monomers can often poison the structure and function of multimeric proteins (the dominant negative effect). Conversely, coexpression of functional monomers of a multimer can often rescue partially defective monomers. We used this reasoning and coexpressed a small amount of WT L1 along with each of the chimeric constructs. We hypothesized that these wild type monomers would relieve steric stress and encourage proper folding and assembly of VLPs. Molecular dynamics simulations done as a supplement to this work seems to suggest that this is the case, with one wild type monomer being included per pentamer, and allowing particle assembly to proceed (see supplemental information). VLP assembly of both of the chimeras was improved by coexpression with WT L1, which preferentially coassembled into the VLPs in a ratio higher than the ratio of coexpression. The migration of these mixed VLPs during rate zonal ultracentrifugation was shifted towards the bottom of the gradient, similar to WT VLPs, probably due to the particles having fewer monomeric units with a FL insert.

The chimeric HPV L1/DENV FL proteins described here self-assemble into VLPs that are potentially attractive multi-pathogen vaccine candidates. For DENV in particular, the focus on a broadly neutralizing epitope may help to solve the problem with ADE faced by current vaccines. We also show two different methods that are useful for stabilizing expression and assembly of chimeric proteins: Design of flanking sequences that can form a disulfide bond to isolate the inserted sequence from the host protein was shown to improve VLP formation. Coexpression with WT L1 resulted in formation of higher levels of mixed VLPs that still contained chimeric monomers. This work extends the successful combination of vaccines, such as the MMR and DTaP, in an effort to produce vaccines that can be provided at lower cost to generate coverage against multiple pathogens in a single dose.

4 | MATERIALS AND METHODS

4.1 | Design of constructs

Multiple HPV-L1 sequence alignments were carried out in UGENE[26] using MUSCLE[27]. Structures were inspected and homology models were constructed using MOE (Molecular Operating Environment, CCG, Montreal). Manual docking was used to position the FL (PDBid 1OAN residues 67-117) in relation to a model of the HPV-L1 capsomere (PDBid 2R5K), followed by loop building using MOE's Loop Modeler function and local energy minimization. The flanking sequences CGP/GPC were added in such a way that the two cysteines were within 6Å and could form a disulfide bond. Genes for all designed constructs were made by Genscript (New Jersey), using the p16L1-GFP plasmid which co-expresses HPV type 16 L1 and GFP[28].

4.2 | Cell culture and transfection

Human embryonic kidney HEK 293TT cells (ATTC, Manassas, VA) were cultured in Dulbecco's Modified Eagle Medium (DMEM) supplemented with 10% (v/v) FBS, 2 mM Glutamax, 100 U/mL penicillin G, 100 µg/mL streptomycin, 0.25 µg/mL amphotericin B, and 250 µg/mL hygromycin B at 37°C with 5% (v/v) CO_2. Cells were transfected in serum free DMEM using Mirus TransIT-293 transfection reagent (Mirus #MIR 2704) according to manufacturer's protocol and incubated at 37°C with 5% (v/v) CO_2 for 4 days. GFP fluorescence was first observed ~48 h post-transfection. Cells were harvested and spun in a clinical centrifuge at 700 rpm for 15 min at 4°C. Cell pellets were re-suspended in 500 µL 2x lysis buffer consisting of 1/10 volume 10% (v/v) Triton X-100, 1/20 volume 1 M ammonium sulfate adjusted to pH 9.0, and 1:500 dilution of Pierce Universal Nuclease for Cell Lysis (Thermo Scientific #88700) in phosphate buffered saline (PBS).

4.3 | Immunofluorescence and confocal microscopy

Confocal microscopy was performed as previously described[20]. HEK 293TT cells were grown until 25% confluent on no. 1.5 Gold Seal coverglass coverslips (Erie Scientific, Portsmouth, NH, USA) in each well of a 6-well plate (Corning, Kennebunk, ME, USA) in complete DMEM without hygromycin. Cells were transfected with plasmids (Genscript, Piscataway, NJ, USA) containing a GFP-expressing reporter gene using Mirus TransIT-293 transfection reagent (Mirus Bio, Madison, WI, USA) and incubated at 37°C with 5% (v/v) CO_2 for 4 days. Cells were fixed in Formalde-Fresh Solution (ThermoFisher) for 1h at RT and permeabilized with 70% (v/v) ethanol for 30 min at RT, rinsing between each step with PBS. Transfected cells were immunostained and incubated overnight at RT with a primary Ab solution containing 2 µg/mL of either anti-HPV16 L1 mouse monoclonal IgG_{2a} Ab CAMVIR-1 (Santa Cruz Biotechnology, Dallas, TX) or anti-DENV hMAb 1.6D[20] in 0.1% (v/v) Tween20 (Sigma-Aldrich, St. Louis, MO), 5% (w/v) non-fat dry milk, and PBS. Secondary Ab solution consisting of 2 µg/mL Alexa Fluor 594-conjugated goat anti-mouse or goat anti-human IgG (H+L) (Invitrogen, Carlsbad, CA) in 0.1% Tween20 and PBS was added and incubated overnight at RT. Nuclei were counterstained with 0.5 µg/mL Hoechst (Cambrex, Walkersville, MD) for 15 min at RT followed by a final rinse step. Fluoromount-G (Southern Biotech, Birmingham, AL) was used to mount coverslips onto Fisherbrand Superfrost microscope slides (Fisher Scientific, Pittsburgh, PA). Images were obtained using an Olympus FV1000 Confocal Microscope System.

4.4 | Maturation and purification of VLPs

Cell lysate was matured by 18-24 hours incubation in a 37°C water bath and clarified by incubation for 10 min on ice followed by the addition of 0.17 volumes of 5M NaCl (85uL/500uL lysate). This solution was spun at 5,000 xg for 10 min at 4°C to pellet debris. The supernatant was transferred to a new 1.5mL tube and spun again.

4.5 | Ultracentrifugation of VLPs

Rate-zonal density gradients were prepared using 60% Optiprep (Sigma #D1556-250ML). 10% and 30% solutions were prepared in Dulbecco's phosphate-buffered saline (DPBS)/0.8M NaCl. Gradients were created using inclined rotation (Gradient Mate, BioComp) in ultracentrifuge tubes (Beckman #349622). 125µL of clarified lysate was added to the top of each gradient tube. Tubes were then spun in an SW50 rotor at 45,000 RPM for 30 min at 20°C. Nine fractions (~525uL each) were collected from the bottom of each tube using a Beckman Fraction Recovery System.

4.5 | HPV L1 SDS-PAGE and Western blots

2-20% precast gels (Biorad) were used for running SDS-PAGE. Samples were prepared by diluting 1:1 in Laemmli buffer with DTT and boiling for 10 minutes. Before loading onto the gel, samples were spun for 1 minute at 10,000 RPM in an Eppendorf microfuge. Gels were run at 100V for 1 hour and 15 minutes in Tris-Glycine-SDS running buffer. Proteins were transferred to a PVDF membrane at 0.3 amps for 1 h 15 min. The membrane was blocked with PBS-T + 3% BSA for 1h at room temperature. Primary anti-HPV 16 L1 antibody (CAMVIR-1, Santa Cruz Biotechnology, Dallas, TX) was added to the membrane diluted 1:500 in PBS-T + 3% BSA and incubated overnight at 4°C. The membrane was then washed for 30 min with PBS-T, followed by secondary antibody (Alexafluor 488 goat anti-mouse) diluted 1:500 in PBS-T at room temperature for 3 h 30 min. The membrane was washed again with PBS-T for 30 min at RT, then dried overnight before scanning.

4.6 | DENV FL enzyme linked immunoassay

Corning brand high-bind 96-well plates (ThermoFisher, Waltham, MA) were coated with 100 µL/well of antigen, either L1-WT VLP or L1-cysFL VLP. Plates were incubated at 4°C for 48 h, equilibrated to room temperature, then rinsed 6x with wash buffer containing 0.5% (v/v) Tween20 (Sigma) in PBS. Wells were blocked with 200 µL blocking buffer containing 5% (w/v) non-fat dry milk and 0.5% (v/v) Tween20 in PBS, incubated at RT for 1 h, and rinsed 6x with wash buffer. Varying concentrations of primary anti-DENV FL HMAb 1.6D (REFS 19, 20 Costin, Schieffelin) were prepared in wash buffer, 100 µL/well was added and incubated at RT for 1 h 30 min, then rinsed 6x with wash buffer warmed to 37°C. Secondary peroxidase-conjugated affinity purified goat anti-human IgG (Pierce, Rockford, IL, USA) was diluted to 2 µg/mL in wash buffer, 100 µL/well was added and incubated covered at RT for 1 h. After a final 37°C wash step, color was developed with tetramethylbenzidine peroxide (ProMega, Madison, WI). The reaction was stopped after 3 min by adding 1M phosphoric acid (Sigma, Saint Louis, MO), and the absorbance was read at 450 nm.

4.7 | Electron microscopy

The VLP fraction collected by ultracentrifugation was desalted by centrifugal filter (Centriprep 30K, Millipore Sigma) to remove Optiprep. 0.5 µL of the desalted VLP fraction was air dried onto a 300 mesh Carbon Type B copper grid (Ted Pella, Redding CA), for approximately 10 minutes, then stained with 0.5 µL 2% uranyl acetate solution for 60 s. Excess stain was blotted away gently. Images were collected using a JEOL 2011 TEM with an accelerating voltage of 200 kV. Images were taken at a nominal magnification of 100,000x.

SUPPLEMENTARY MATERIALS

The following are provided for additional depth. Supplementary Figure 1. Multiple sequence alignment and phylogram for 23 mutually diverse primate papilloma virus L1 sequences, showing sites of high variability. Supplementary Figure 2. An illustration of greek-key, jelly roll protein folding pathway and assembly of the capsomeres and VLPs, showing loop intercalation. Supplementary Figure 3. Blow-up image of the modeled cysFL insertion, near the 5-fold axis of the capsomere. Supplementary Figure 4. Relative staining of HPVL1-WT and HPVL1-FL by conformational antibodies to the FL. Supplementary Figure 5. Wild-type HPVL1 tetramer. Supplementary Figure 6. HPVL1-cysFL tetramer. Supplementary Video 1. Molecular dynamics simulation of the wild-type HPVL1 tetramer. Supplementary Video 2. Molecular dynamics simulation of the HPVL1-cysFL tetrameric state.

ACKNOWLEDGEMENTS

The Authors declare that there is no conflict of interest. This work was supported by NIH R01GM099827-01A1 to CB and SFM. We would like to express our thanks to John Schiller for helpful discussions and the HPV L1 expression system.

AUTHOR CONTRIBUTIONS

Danielle A. Basore: Data curation; investigation; methodology; validation; visualization; writing-original draft; writing-review and editing.
Carolyn M. Barcellona: Data curation; investigation; methodology; validation; visualization; writing-original draft; writing-review and editing.
Thomas B. Jordan: Data curation; investigation; methodology; validation; visualization; writing-review and editing.
Donna E. Crone: Methodology; validation; writing-review and editing.
Christopher Bystroff: Conceptualization; data curation; investigation; methodology; project administration; validation; visualization; writing-original draft; writing-review and editing.
Scott F. Michael: Conceptualization; data curation; methodology; project administration; validation; visualization; writing-original draft; writing-review and editing

FIGURE 1 (a) Design of 558-residue HPV16-L1 chimeras with inserted 58-residue DENV FL sequences inserted into the DE loop, replacing Ala-Asn (red). The cysFL insert contains flanking CGP/GPC motif for improved stability (green), while FL has a single Gly. Native disulfide-forming cysteines are shaded (cyan, intramolecular; yellow, intermolecular) (b) Modeled structure of chimeric HPV16 L1 monomer and capsomere, based on crystal structures of HPV11-L1 (PDBid:2R5K) and DENV2 E-protein (PDBid:3C5X), showing the FL or cysFL in black.

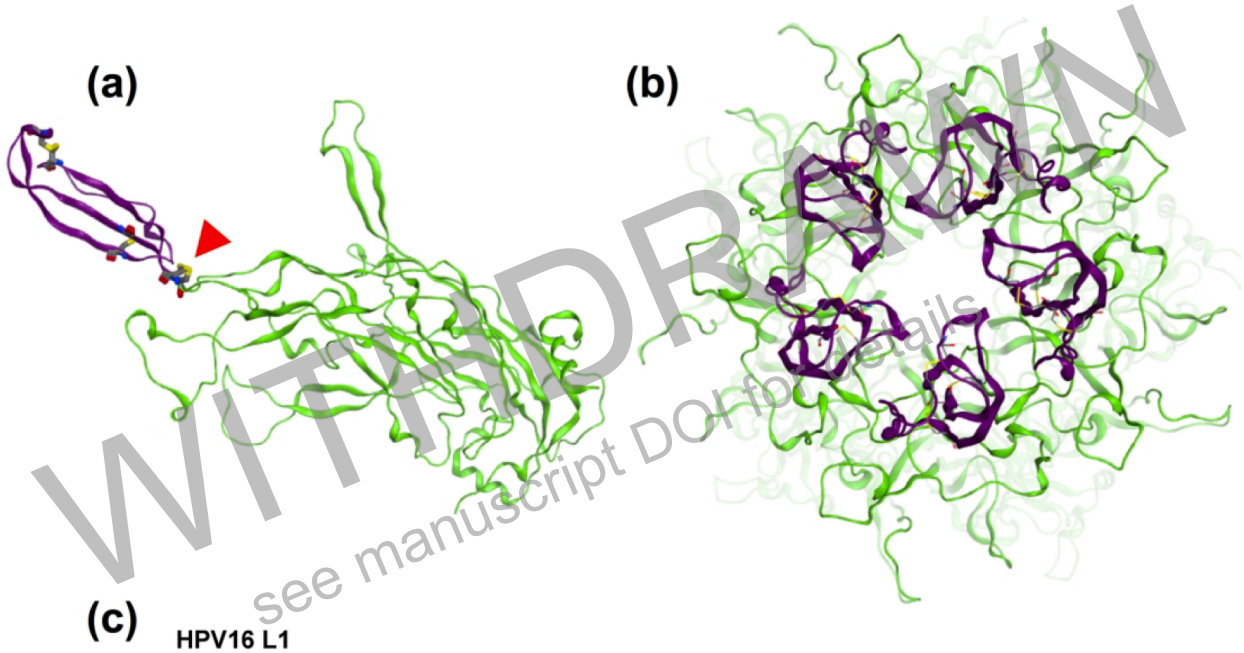

(c)

HPV16 L1

MSLWLPSEATVYLPPVPVSKVVSTDEYVARTNIYYHAGTSRLLAVGHPYFPIKKPNNNK
ILVPKVSGLQYRVFRIHLPDPNKFGFPDTSFYNPDTQRLVWACVGVEVGRGQPLGVGIS
GHPLLNKLDDTENASAYAANAGVDNRECISMDYKQTQLCLIGCKPPIGEHWGKGSPCTN
VAVNPGDCPPLELINTVIQDGDMVDTGFGAMDFTTLQANKSEVPLDICTSICKYPDYIK
MVSEPYGDSLFFYLRREQMFVRHLFNRAGTVGENVPDDLYIKGSGSTANLASSNYFPTP
SGSMVTSDAQIFNKPYWLQRAQGHNNGICWGNQLFVTVVDTTRSTNMSLCAAISTSETT
YKNTNFKEYLRHGEEYDLQFIFQLCKITLTADVMTYIHSMNSTILEDWNFGLQPPPGGT
LEDTYRFVTSQAIACQKHTPPAPKEDPLKKYTFWEVNLKEKFSADLDQFPLGRKFLLQA
GLKAKPKFTLGKRKATPTTSSTSTTAKRKKRKL

DENV inserts

FL

GITNTTTDSRCPTQGEPTLNEEQDQNFVCKHTMVDRGWGNGCGLFGKGGLVTCAMFG

cysFL

CGPNTTTESRCPTQGEPTLNEEQDKRFVCKHSMVDRGWGNGCGLFGKGGIVTCAGPC

FIGURE 2 Expression of chimeric proteins in transfected cells. Western blot of relative expression levels of wild type HPV16 L1 and the two chimeric constructs with a consensus DENV FL and with a DENV2 FL and a cysteine disulfide lock (cysFL). The L1 protein is detected using an anti-L1 mouse monoclonal Ab. Untransfected cell lysate is run as a negative control. 50 and 75 kD size standards are indicated. WT L1 is expressed at a higher level than either chimera. The chimeric L1 proteins are slightly larger than the WT protein.

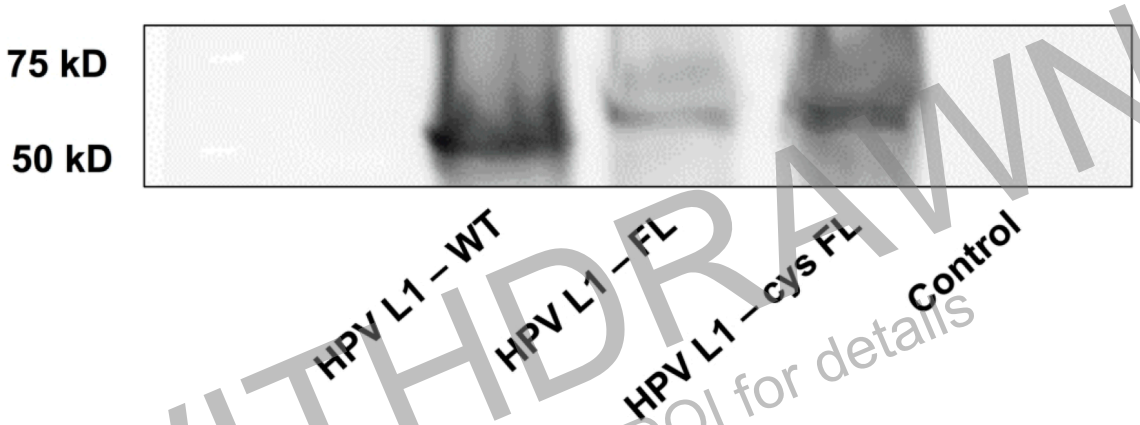

FIGURE 3 Immunofluorescence microscopy of transfected cells (400X magnification). L1 protein (red) is detected using an anti-L1 mouse monoclonal Ab. GFP (green) is co-expressed from the transfected plasmid. Nuclei are counterstained blue. Untransfected cells are shown as a negative control.

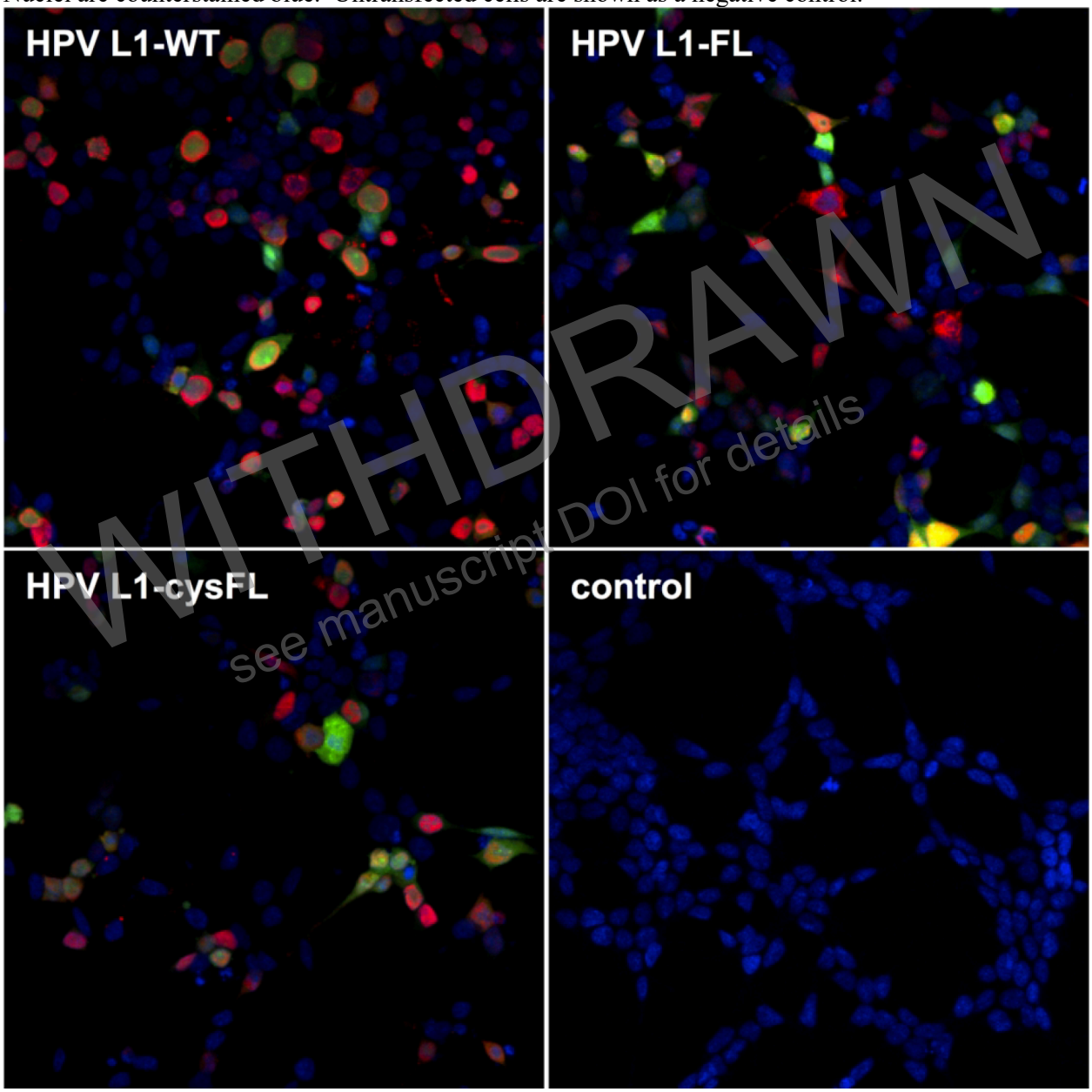

FIGURE 4 Assembly of chimeric virus like particles. Western blots of fractions from rate zonal centrifugation of matured, transfected cell lysates. WT L1, the consensus FL and the DENV2 FL with the disulfide (cysFL) were compared. Additionally, matured lysates from cell transfected with a 9:1 ratio of chimeric to WT L1 were compared to evaluate the ability of WT L1 to rescue assembly of chimeras. The L1 protein is detected using an anti-L1 mouse monoclonal Ab. 50 kD size standards are indicated. Assembled VLPs migrate into the center fractions. The chimeric L1 proteins are slightly larger than the WT L1 protein.

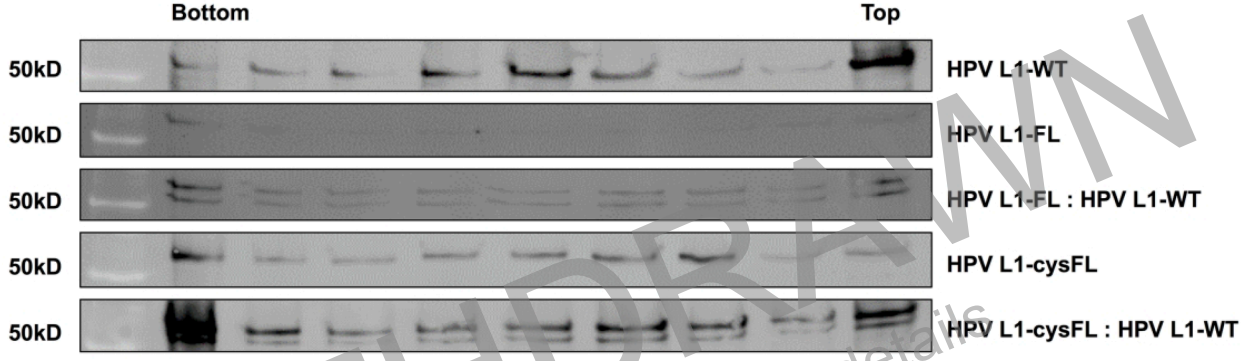

336 **FIGURE 5** Transmission Electron Micrograph images of (a) assembled HPV16 L1-WT, (b) HPV16 L1-
337 cysFL and (c) HPV18 L1-WT. Samples were air dried onto grid and stained with uranyl acetate. 50 nm
338 scale bars are shown.

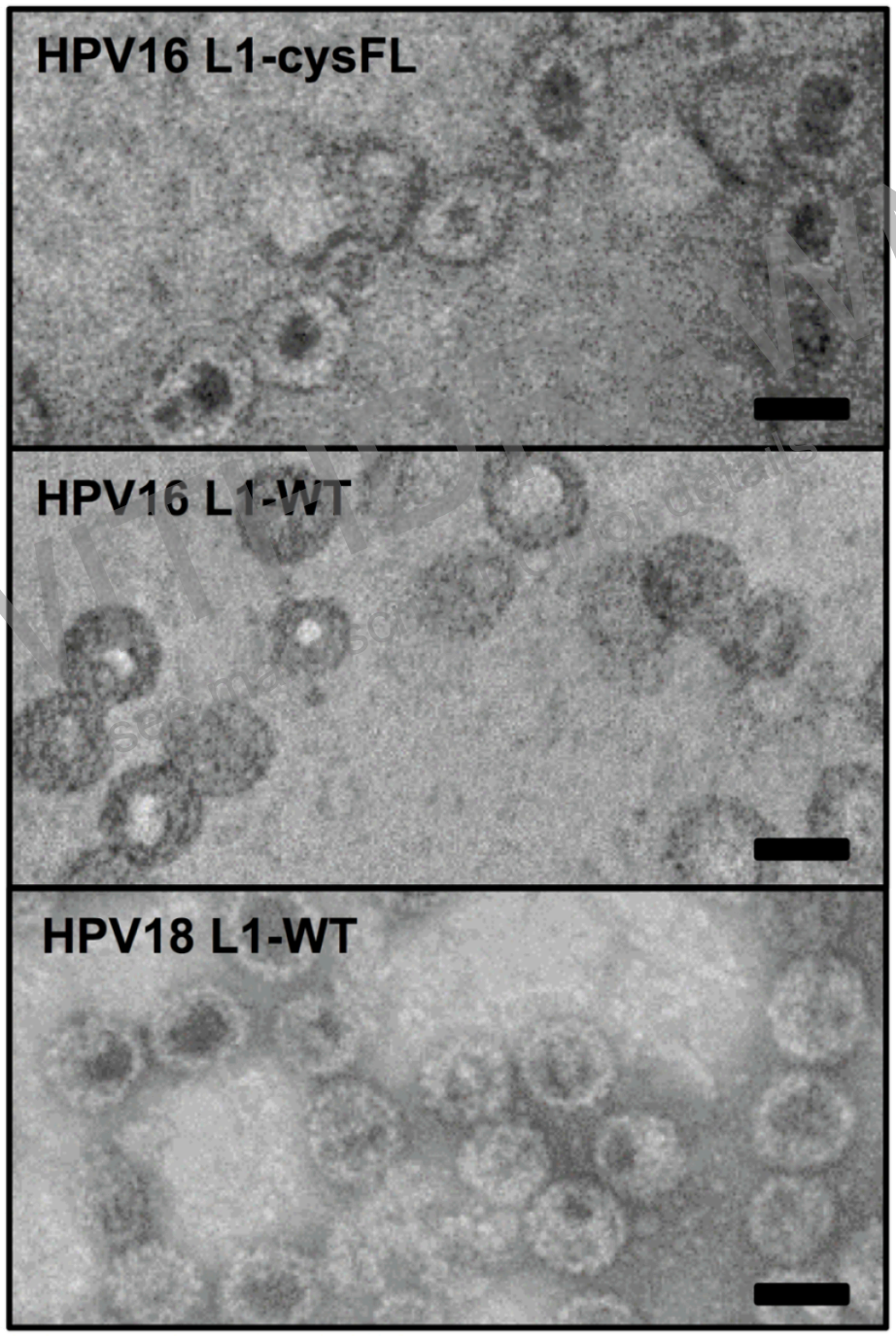

339
340

FIGURE 6 The DENV FL can be detected on assembled VLPs using a conformationally-sensitive human monoclonal Ab. Equalized quantities of assembled WT L1 and cysteine locked FL L1 VLPs were probed by ELISA using a conformationally-sensitive human monoclonal Ab against the fusion loop. This Ab specifically detected the FL containing chimeric VLPs, but did not react with the WT L1 VLPs.

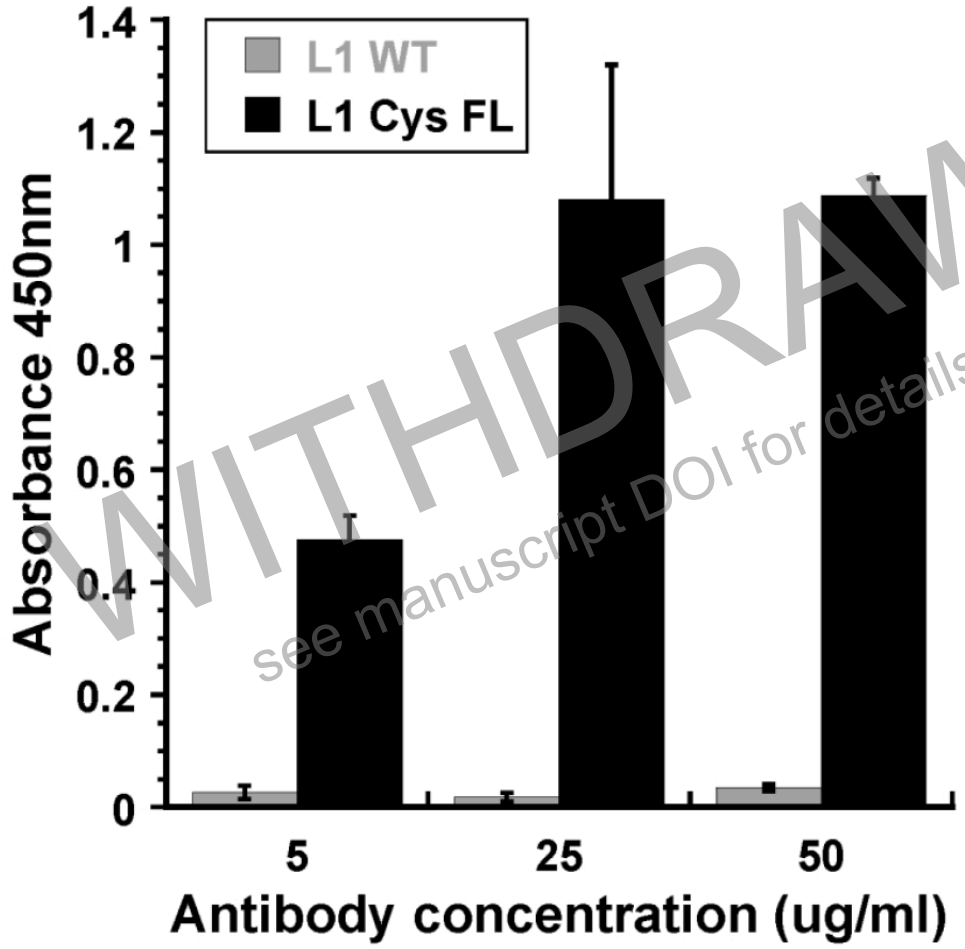

REFERENCES

1. Denis J, Majeau N, Acosta-Ramirez E, Savard C, Bedard M-C, Simard S, Lecours K, Bolduc M, Pare C, Willems B, et al. (2007) Immunogenicity of papaya mosaic virus-like particles fused to a hepatitis C virus epitope: Evidence for the critical function of multimerization. Virology [Internet] 363:59–68. Available from: https://www.sciencedirect.com/science/article/pii/S004268220700027X

2. Miura K, Stone WJR, Koolen KM, Deng B, Zhou L, van Gemert G-J, Locke E, Morin M, Bousema T, Sauerwein RW, et al. (2016) An inter-laboratory comparison of standard membrane-feeding assays for evaluation of malaria transmission-blocking vaccines. Malar. J. [Internet] 15:463. Available from: http://malariajournal.biomedcentral.com/articles/10.1186/s12936-016-1515-z

3. Seitz H, Dantheny T, Burkart F, Ottonello S, Müller M (2013) Influence of oxidation and multimerization on the immunogenicity of a thioredoxin-l2 prophylactic papillomavirus vaccine. Clin. Vaccine Immunol. [Internet] 20:1061–9. Available from: http://www.ncbi.nlm.nih.gov/pubmed/23677323

4. Yan M, Peng J, Jabbar IA, Liu X, Filgueira L, Frazer IH, Thomas R (2005) Activation of dendritic cells by human papillomavirus-like particles through TLR4 and NF-κB-mediated signalling, moderated by TGF-β. Immunol. Cell Biol. [Internet] 83:83–91. Available from: https://onlinelibrary.wiley.com/doi/10.1111/j.1440-1711.2004.01291.x

5. Yu SS, Lau CM, Thomas SN, Jerome WG, Maron DJ, Dickerson JH, Hubbell JA, Giorgio TD (2012) Size- and charge-dependent non-specific uptake of PEGylated nanoparticles by macrophages. Int. J. Nanomedicine [Internet] 7:799. Available from: http://www.ncbi.nlm.nih.gov/pubmed/22359457

6. Victora GD, Nussenzweig MC (2012) Germinal Centers. Annu. Rev. Immunol. [Internet] 30:429–457. Available from: https://www.annualreviews.org/doi/10.1146/annurev-immunol-020711-075032

7. Schiller JT, Lowy DR (1996) Papillomavirus-like particles and HPV vaccine development. Semin. Cancer Biol. [Internet] 7:373–382. Available from: https://www.sciencedirect.com/science/article/abs/pii/S1044579X96900462

8. Stanley M (2008) Immunobiology of HPV and HPV vaccines. Gynecol. Oncol. [Internet] 109:S15–S21. Available from: https://www.sciencedirect.com/science/article/pii/S0090825808001054?casa_token=eBt7UXG8qbQAAAAA:x4OVjWKwDiTUMGEPjv9Q4e3yoirjv5NM5nHBdSCZNpDp66KJkWu68perYIlq6OYZ0gxzwJfjEA

9. McLemore MR (2006) Gardasil®: Introducing the New Human Papillomavirus Vaccine. Clin. J. Oncol. Nurs. [Internet] 10:559–560. Available from: http://cjon.ons.org/cjon/10/5/gardasil®-introducing-new-human-papillomavirus-vaccine

10. Schellenbacher C, Roden R, Kirnbauer R (2009) Chimeric L1-L2 virus-like particles as potential broad-spectrum human papillomavirus vaccines. J. Virol. [Internet] 83:10085–95. Available from: http://www.ncbi.nlm.nih.gov/pubmed/19640991

11. Skolnick J, Kolinski A (1990) Dynamic Monte Carlo simulations of globular protein folding/unfolding pathways: I. Six-member, Greek key β-barrel proteins. J. Mol. Biol. [Internet] 212:787–817. Available from: https://www.sciencedirect.com/science/article/pii/002228369090237G

12. Capaldi AP, Ferguson SJ, Radford SE (1999) The greek key protein apo-pseudoazurin folds through an obligate on-pathway intermediate. J. Mol. Biol. [Internet] 286:1621–1632. Available from:

https://www.sciencedirect.com/science/article/pii/S0022283698925888?casa_token=FNz9e-KI2vkAAAAA:uEJmPvoA_ceR1DDhqzQ-o0RomNa6rOOUv-gnOrDgnpk73s2DBovOpCdr-yTWA0nRPc4NuGX55A

13. Bork P, Holm L, Sander C (1994) The Immunoglobulin Fold: Structural Classification, Sequence Patterns and Common Core. J. Mol. Biol. [Internet] 242:309–320. Available from: https://www.sciencedirect.com/science/article/pii/S0022283684715828

14. Efimov A V. (1997) Structural trees for protein superfamilies. Proteins Struct. Funct. Genet. [Internet] 28:241–260. Available from: https://onlinelibrary.wiley.com/doi/10.1002/(SICI)1097-0134(199706)28:2%3C241::AID-PROT12%3E3.0.CO;2-I

15. Schellenbacher C, Roden R, Kirnbauer R (2009) Chimeric L1-L2 Virus-Like Particles as Potential Broad-Spectrum Human Papillomavirus Vaccines. J. Virol. 83:10085–10095.

16. Palatnik-de-Sousa CB, Soares I da S, Rosa DS (2018) Editorial: Epitope Discovery and Synthetic Vaccine Design. Front. Immunol. [Internet] 9:826. Available from: http://journal.frontiersin.org/article/10.3389/fimmu.2018.00826/full

17. Bente DA, Rico-Hesse R (2006) Models of dengue virus infection. Drug Discov. Today Dis. Model. [Internet] 3:97–103. Available from: https://www.sciencedirect.com/science/article/pii/S1740675706000156?casa_token=ZKr3Hzk8FkQAAAAA:eYGAZpjjbV5oFlImq0Hhyr9IYvrn39DtcAq5gjOpc717HVqqJbZnsBbF9_c0NChnsn-m1kH-3g

18. Bhatt S, Gething PW, Brady OJ, Messina JP, Farlow AW, Moyes CL, Drake JM, Brownstein JS, Hoen AG, Sankoh O, et al. (2013) The global distribution and burden of dengue. Nature [Internet] 496:504–507. Available from: http://www.nature.com/articles/nature12060

19. Halstead SB (2017) Dengvaxia sensitizes seronegatives to vaccine enhanced disease regardless of age. Vaccine [Internet] 35:6355–6358. Available from: https://www.sciencedirect.com/science/article/pii/S0264410X17313610?casa_token=k22wjIk97nMAAAAA:ZSnG6bqGED1NSfAgghgxF7G2_pHBbRNgXaUHr4aaEIV38WP-25pxWInVQ0B9SgsE63ot-iBbBw

20. Costin JM, Zaitseva E, Kahle KM, Nicholson CO, Rowe DK, Graham AS, Bazzone LE, Hogancamp G, Figueroa Sierra M, Fong RH, et al. (2013) Mechanistic Study of Broadly Neutralizing Human Monoclonal Antibodies against Dengue Virus That Target the Fusion Loop. J. Virol. [Internet] 87:52–66. Available from: https://journals.asm.org/doi/10.1128/JVI.02273-12

21. Schieffelin JS, Costin JM, Nicholson CO, Orgeron NM, Fontaine KA, Isern S, Michael SF, Robinson JE (2010) Neutralizing and non-neutralizing monoclonal antibodies against dengue virus E protein derived from a naturally infected patient. Virol. J. [Internet] 7:28. Available from: https://virologyj.biomedcentral.com/articles/10.1186/1743-422X-7-28

22. Huang CY-H, Butrapet S, Moss KJ, Childers T, Erb SM, Calvert AE, Silengo SJ, Kinney RM, Blair CD, Roehrig JT (2010) The dengue virus type 2 envelope protein fusion peptide is essential for membrane fusion. Virology [Internet] 396:305–315. Available from: https://www.sciencedirect.com/science/article/pii/S0042682209006515

23. Lu Z, Murray KS, Cleave V Van, LaVallie ER, Stahl ML, McCoy JM (1995) Expression of Thioredoxin Random Peptide Libraries on the Escherichia coli Cell Surface as Functional Fusions to Flagellin: A System Designed for Exploring Protein-Protein Interactions. Nat. Biotechnol. [Internet] 13:366–372. Available from: http://www.nature.com/doifinder/10.1038/nbt0495-366

24. Matsumura M, Signor G, Nature BM-, 1989 undefined Substantial increase of protein stability by multiple disulphide bonds. nature.com [Internet]. Available from:

https://idp.nature.com/authorize/casa?redirect_uri=https://www.nature.com/articles/342291a0&casa_token=4OdqHpl8xjAAAAAA:6D6gz33cPKKqgTNjY2NHlq5Ls_BcJhhai3dDwxzV37xlKCDJVhA3dILUuq-0wMImX4pFe9Ck9mKY4LwJ

25. Fersht AR (2000) Transition-state structure as a unifying basis in protein-folding mechanisms: contact order, chain topology, stability, and the extended nucleus mechanism. Proc. Natl. Acad. Sci. U. S. A. [Internet] 97:1525–9. Available from: http://www.ncbi.nlm.nih.gov/pubmed/10677494

26. Okonechnikov K, Golosova O, Fursov M (2012) Unipro UGENE: a unified bioinformatics toolkit. Bioinformatics [Internet] 28:1166–1167. Available from: https://academic.oup.com/bioinformatics/article-lookup/doi/10.1093/bioinformatics/bts091

27. Edgar RC (2004) MUSCLE: multiple sequence alignment with high accuracy and high throughput. Nucleic Acids Res. [Internet] 32:1792–7. Available from: http://www.ncbi.nlm.nih.gov/pubmed/15034147

28. Buck CB, Pastrana D V., Lowy DR, Schiller JT Generation of HPV Pseudovirions Using Transfection and Their Use in Neutralization Assays. In: Human Papillomaviruses. New Jersey: Humana Press; 2005. pp. 445–462. Available from: http://link.springer.com/10.1385/1-59259-982-6:445